Journal of Water Process Engineering 15 (2017) 89–98

Contents lists available at ScienceDirect

Journal of Water Process Engineering

journal homepage: www.elsevier.com/locate/jwpe

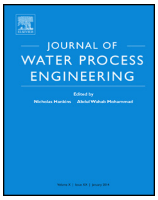

Fouling behaviours of PVDF-TiO_2 mixed-matrix membrane applied to humic acid treatment

Y.H. Teow[a,b,*], B.S. Ooi[c], A.L. Ahmad[c]

[a] Centre for Sustainable Process Technology (CESPRO), Faculty of Engineering and Built Environment, Universiti Kebangsaan Malaysia, 43600 Bangi, Selangor, Malaysia
[b] Department of Chemical and Process Engineering, Faculty of Engineering and Built Environment, Universiti Kebangsaan Malaysia, 43600 Bangi, Selangor, Malaysia
[c] School of Chemical Engineering, Engineering Campus, Universiti Sains Malaysia, Seri Ampangan, 14300 Nibong Tebal, Penang, Malaysia

ARTICLE INFO

Article history:
Received 20 December 2015
Received in revised form 7 March 2016
Accepted 11 March 2016
Available online 3 April 2016

Keywords:
Fouling mechanism
Humic acid
Mixed-matrix membrane
TiO_2 nanoparticles
Ultrafiltration

ABSTRACT

The aim of this study was to analyses the fouling mechanism of polyvinylidene fluoride-titanium dioxide (PVDF-TiO_2) mixed-matrix membranes (MMMs) embedded with three different types of TiO_2 nanoparticles (NPs): PC-20, P25, and X500 applied to humic acid (HA) treatment. Although neat membrane has very often been used in a model adapted to cross-flow ultrafiltration (UF), MMM with TiO_2 embedment has not been studied before. The identification of fouling mechanisms was determined by four typical modes of Hermia's models and the combined blocking model. The combined blocking model, which involves both cake filtration and pore blocking, taking place at different stages of the membrane filtration process, shows the best correlation with the experimental data. It was shown that the fouling behaviour of the membrane is governed by the nature of the membrane, especially membrane surface roughness. The fine and well dispersed X500 NPs on membrane polymeric matrix were found to have a significant effect on membrane anti-fouling property with a reduced pore blocking parameter, lowest cake layer resistance, and membrane resistance of 0.3261, 2.6201×10^6/m, and 10.2182×10^6/m respectively. This finding is attributed to the reduced surface roughness as well as increasing surface energy of X500 MMM.

1. Introduction

The presence of humic acid (HA) in the environment can lead to detrimental problems due to the formation of harmful disinfection by-products (DBPs) [1,2] when it undergoes conventional chlorine treatment processes. Progress has been made with regards to the extensive use of ultrafiltration (UF) membranes as an alternative technology to conventional treatment in separating HA particles from the water source to meet more stringent water quality regulations [3,4]. However, despite the expansion and successful application of membrane systems in the water industry, a decline in membrane performance over a period of time due to membrane fouling is still a critical problem. It demands considerable attention as it causes a decline in permeate flux, affects separation properties, and increases the operational pressure [5,6], thus constraining the widespread application of membrane technology for HA separation in water treatment processes.

HA fouling can involve several distinct phenomena. Yamamura et al. [7] classified membrane fouling as physically reversible fouling (concentration polarization), which can be totally eliminated by physical cleaning or certain pre-treatment, and physically irreversible fouling (HA adsorption and deposition), which cannot be entirely counteracted by physical cleaning or certain pre-treatment [8,9]. Visvanathan and Ben aïm [10] suggested that in the early stage of filtration, there is a sharp decline in permeate flux which is irreversible for all practical purposes due to the rapid deposition of fine particles from suspension on the membrane surface and subsequently penetrate into the pores and thus accumulate. Later, aggregates of colloids can form bridges over the pore openings, resulting in partial blocking of the pores. A smaller pore structure is then available for subsequent colloids to deposit. The bridging of aggregated colloids leads to the eventual formation of a film of colloids on the membrane surface, which implies that more than one type of blocking mechanism is involved in a single process. This postulation is in good agreement with the findings of Tarleton and Wakeman [11] who claimed that the fouling by particulates appears to be caused by several simultaneous mechanisms.

---

[*] Corresponding author at: Centre for Sustainable Process Technology (CESPRO), Faculty of Engineering and Built Environment, Universiti Kebangsaan Malaysia, 43600 Bangi, Selangor, Malaysia.
E-mail addresses: yh_teow@ukm.edu.my, yeithaan@yahoo.com (Y.H. Teow).

http://dx.doi.org/10.1016/j.jwpe.2016.03.005
2214-7144/© 2016 Elsevier Ltd. All rights reserved.

In contrast, Cakl and Mikulášek [12] concluded that the fouling mechanism is highly dependent on solute particle size and membrane pore size. They observed that cake formation takes place if the particles are larger than the pores, whereas partial blocking occurred when membrane pore size was very close to the diameter of the particles filtered; this concurred with the report by Dal-Cin et al. [13].

In this work, four empirical models to describe permeate flux declined (pore blocking – complete, intermediate and standard; and cake layer formation) presented by Hermia [14] were used to fit the experimental results in quantifying the membrane properties on membrane fouling and to identify the fouling mechanism involved for the economic and technological point view of membrane treatment process in separating HA. By elucidating the fouling mechanism, one can adapt the hydrodynamic process to control membrane fouling. While most of the studies performed by other researchers in identifying the fouling mechanism reported on neat membranes, polyvinylidene fluoride-titanium dioxide (PVDF-TiO_2) mixed-matrix membranes (MMMs) with three different commercial TiO_2 nanoparticles (NPs), P25, PC-20, and X500 were considered in this study. Additionally, as a single type of fouling mechanism appears to be rare, since there is usually a range of size distribution in both membrane pores and filtered molecules, a dynamic combined blocking model was further employed to interpret the fouling behaviour.

2. Theoretical background

2.1. Modelling and mechanism of fouling

To identify the possible dominant mechanism of membrane fouling, we followed the work reported by Hermans and Bredée [15]. Hermans and Bredée [15] showed that for all of the classical models of flux decline during constant transmembrane pressure (TMP), the flux changes over the time can be identified by the following unique mathematical expression:

$$\frac{d^2t}{dV^2} = \beta\left(\frac{dt}{dV}\right)^n \tag{1}$$

where V is the cumulative filtrate volume, t is the filtration time and β is a proportionality constant. The permeate flux is expressed as [16]:

$$J = \frac{1}{A}\frac{dV}{dt} \tag{2}$$

Eq. (2) can be expressed as the first derivative, $dt/dV = 1/AJ$, simply the inverse of the instantaneous filtrate flow rate while the second derivation of this equation with respect to t, $d^2t/dV^2 = -(1/AJ^3)\ dJ/dt$, is proportional to the rate of increase in the total resistance to filtration. By substituting both equations into Eq. (1), it leads to the governing equation of flux decline with time:

$$\frac{dJ}{dt} = -\alpha J^{3-n} \tag{3}$$

where α is a constant.

A fouling correlation was made by Field et al. [17] according to the classical constant pressure dead end filtration equation [15] as:

$$\frac{dJ}{dt} = -K(J - J^*)J^{(2-n)} \tag{4}$$

where J^* is the steady state flux and K is constant depends on n dimension values. n is a general index used to distinguish different fouling mechanisms [18]. Fig. 1 illustrates the different fouling mechanisms and the sub-section below provides various blocking mechanisms model equations for flux reduction at constant filtration pressure.

2.1.1. Complete pore blocking (n = 2)

In the complete pore blockage mode, the flux was shut off by solute aggregates that are larger than the pore size, depositing on the membrane surface and decrease in the available pores without any superposition, whereby filtrate can only pass through the unblocked pore area. The model was derived by substituting $n = 2$ in Eq. (4) and integrating with the time of permeate flux [19]:

$$\ln\left(\frac{1}{J}\right) = \ln\left(\frac{1}{J_0}\right) + k_1 t \tag{5}$$

2.1.2. Pore constriction (n = 1.5)

The pore restriction mode accounts for fouling that occurs in the internal structure of the membrane. In the pore restriction mode, membranes are assumed to have a set of straight capillaries pores conforming to Poiseuille flow. The membrane pore radius reduction is due to the solute adsorption or deposition to the internal membrane pores walls, thereby constricting its diameter. The exponent is put with the value of $n = 1.5$ and integrating Eq. (4), the permeate flux is decreased and is related to time using the equation expressed as [19]:

$$\frac{1}{\sqrt{J}} = \frac{1}{\sqrt{J_0}} + k_2 t \tag{6}$$

2.1.3. Intermediate pore blocking (n = 1)

The intermediate pore blockage mode is similar to the complete pore blockage model, in addition to accounting for the possibility of particles bridging a pore by obstructing the entrance without completely blocking it [18]. This model substitutes $n = 1$ in Eq. (4); integrating this, the equation is [19]:

$$\frac{1}{J} = \frac{1}{J_0} + k_3 t \tag{7}$$

2.1.4. Cake filtration (n = 0)

In contrast to the pore restriction and pore blocking mode, for the cake filtration model, fouling occurs through the formation of a bed of solute over the entire membrane upper surface, and this fouling layer is permeable to fluid flow with resistance. The overall resistance consists of the cake resistance and the membrane resistance, which is assumed to remain unchanged [18]. The cake filtration model was obtained by substituting the value of $n = 0$ and integrating Eq. (4), the equation is expressed as follows [19]:

$$\frac{1}{J^2} = \frac{1}{{J_0}^2} + k_4 t \tag{8}$$

where in Eq. (5)–(8), J_0 is the initial permeate flux, and k_1-k_4 are the rate of pore blocking.

2.2. Combined blocking models

It is commonly recognised that cross-flow impacts less fouling at the initial stage and at the gel layer (or equivalently filter cake) growing stage. In view of this, Yuan et al. [20] developed a dynamic model to interpret fouling behaviour of cross-flow UF by taking into account two simultaneous fouling phenomena: pore blocking and cake formation [21] in the same mathematical equation. They successfully applied the model in a HA fouling study [22] and protein effluent [21] for the description of permeate flux decline, which is:

$$\frac{J_p}{J_0} = \left\{\left[1 - \left(\exp\left(-\frac{\alpha\cdot\Delta P\cdot C_f}{\mu\cdot R_m}\cdot t\right)\right)\right]\frac{R_m}{(R_m + R_c)} + \left[\exp\left(-\frac{\alpha\cdot\Delta P\cdot C_f}{\mu\cdot R_m}\cdot t\right)\right]\right\} \tag{9}$$

where J_p is the permeate flux, α is the pore blocking parameter, ΔP is the TMP, C_f is the feed concentration, t is time, μ is the dynamic viscosity of the permeate, R_m is the membrane hydraulic resistance,